Initial value problem for magnetic fields in heavy ion collisions

Kirill Tuchin

Initial value problem for magnetic field in heavy ion collisions

Kirill Tuchin[1]

[1] *Department of Physics and Astronomy, Iowa State University, Ames, Iowa, 50011, USA*
(Dated: December 23, 2015)

When the quark-gluon plasma emerges in the wake of a heavy-ion collision, magnetic field created by the valence charges has already permeated the entire interaction region. Evolution of this "initial" field in plasma is governed by the Maxwell equations in electrically conducting medium. As the plasma expands external valence charges induce magnetic field that also contributes to the total magnetic field in plasma. I solve the initial value problem describing these processes and argue that the initial magnetic field often dominates over the one induced by the valence charges. In particular, it grows approximately proportional to the collision energy, unlike the induced component, which is energy-independent. As a result, magnetic field has a significant phenomenological influence on quark-gluon plasma at the LHC energies over its entire lifetime.

I.   INTRODUCTION

In this paper I reexamine the problem of magnetic field created by electrical currents of colliding relativistic heavy ions [1–8]. Since these currents experience very little deflection in the course of collision [9, 10] (and thus have large absolute values of rapidity), the corresponding magnetic field depends on energy and geometry of the collision, and implicitly on the strong interaction dynamics through the electrical conductivity of the quark-gluon plasma (QGP) [2, 6]. Another important aspect, which is the main focus of this study, is the transition dynamics from magnetic field in vacuum to the one in medium. To begin with, assume that QGP forms instantly at time $t = t_0$, where t is counted from the collision time in the laboratory frame. This time emerges in phenomenological models of QGP that favor rather small values as compared to the perturbation theory expectations, see e.g. [11]. The earliest possible value of t_0 is determined by the saturation momentum Q_s as $1/Q_s$ and represents the time it takes to release most particles from the ion's wave functions. At RHIC $1/Q_s \sim 0.2$ fm. At $t < t_0$ we are dealing with electromagnetic field created by the valence charges in vacuum. Its magnetic component is given by the well-known formula (7). At time $t = t_0$, when the QGP emerges, magnetic field permits the entire plasma. Starting at $t = t_0$ and on behavior of magnetic field is governed by the Maxwell equations in plasma. These equations describe evolution of magnetic field in electrically conducting QGP starting from its initial value at $t = t_0$. This component of the total magnetic field is referred to below as the "initial" magnetic field $\boldsymbol{B}_{\text{init}}$. Another contribution to magnetic field is induced by valence charges moving *outside* of QGP and is referred to below as the "valence" contribution $\boldsymbol{B}_{\text{val}}$.* In the previous publications the role of the initial field has not been properly recognized. In this paper I fill this void and moreover, argue that in most cases the main contribution stems from the initial field.

The paper is organized as follows. In Sec. II–Sec. IV I deal with magnetic field produced by a single point charge. In Sec. II I consider magnetic field in vacuum, while in later sections – in electrically conducting QGP. The main result is given by equations (34), (35) which represent contributions of valence charges and the initial field respectively. A more realistic geometry is considered in Sec. V where I discuss the case of two electric charges colliding at a given impact parameter b. I also discuss there the effect of time dependent electrical conductivity on the magnetic field evolution. I discuss the results and summarize in Sec. VI.

II.   MAGNETIC FIELD IN VACUUM

In a relativistic heavy-ion collision, electromagnetic field is created by Z electric charges of one ion and Z electric charges of another ion moving in the opposite directions along, say, z axis such that ion centers are at a distance b away. Due to the superposition principle, the total classical field is a sum of fields of all charges. Thus, in order to find the total field it is sufficient to solve for a single electric charge e. In this section I briefly review a textbook case of electromagnetic field created in vacuum by a uniformly moving point charge e. Our intent here is to introduce notations, definitions etc.

---

* To avoid confusion I emphasize that both components are ultimately related to electrical charges of heavy-ions. The distinction only concerns our treatment of magnetic field at $t > t_0$ as will be explained in detail in the forthcoming sections.

Before the QGP formation, viz. at $t \leq t_0$, the vector potential $\boldsymbol{A}_1(\boldsymbol{r}, t)$ of a point charge e moving along the trajectory $z = vt$ satisfies the following equation

$$\nabla^2 \boldsymbol{A}_1(\boldsymbol{r}, t) = \partial_t^2 \boldsymbol{A}_1(\boldsymbol{r}, t) - \boldsymbol{j}(\boldsymbol{r}, t), \tag{1}$$

where the electromagnetic current density due to a valence charge e is

$$\boldsymbol{j} = ev\hat{\boldsymbol{z}}\delta(z - vt)\delta(\boldsymbol{b}). \tag{2}$$

The momentum space representation is defined as follows

$$\boldsymbol{j}(\boldsymbol{r}, t) = \int \frac{d^3k}{(2\pi)^3} e^{i\boldsymbol{k}\cdot\boldsymbol{r}} \boldsymbol{j}_{\boldsymbol{k}\omega} = \int \frac{d^2k_\perp dk_z}{(2\pi)^3} e^{i\boldsymbol{k}_\perp \cdot \boldsymbol{b} + ik_z z} \boldsymbol{j}_{\boldsymbol{k}\omega}. \tag{3}$$

With this normalization the Fourier component of the current reads

$$\boldsymbol{j}_{\boldsymbol{k}} = ev\hat{\boldsymbol{z}} e^{-ik_z vt}. \tag{4}$$

It follows from (1) that the vector potential generated by the current (4) is

$$\boldsymbol{A}_{1\boldsymbol{k}} = \frac{2\pi ev\hat{\boldsymbol{z}}}{k^2 - k_z^2 v^2} = \frac{2\pi ev\hat{\boldsymbol{z}}}{k_z^2/\gamma^2 + k_\perp^2}. \tag{5}$$

In the configuration space I obtain

$$\boldsymbol{A}_1(\boldsymbol{r}, t) = \frac{\gamma ev\hat{\boldsymbol{z}}}{4\pi} \frac{1}{\sqrt{b^2 + \gamma^2(vt - z)^2}}, \tag{6}$$

where $\gamma = (1 - v^2)^{-1/2}$. The corresponding magnetic field

$$\boldsymbol{B}_1 = -\partial_b A_1 \hat{\boldsymbol{\phi}} = \frac{\gamma ev\hat{\boldsymbol{\phi}}}{4\pi} \frac{b}{(b^2 + \gamma^2(vt - z)^2)^{3/2}}. \tag{7}$$

This solution is valid until $t = t_0$ at which time existence of electrically conducting medium must be taken into account.

III. EXACT SOLUTION FOR CONSTANT ELECTRICAL CONDUCTIVITY

Maxwell equations can be solved exactly for $t \geq t_0$ in the case of constant electrical conductivity σ. The vector potential $\boldsymbol{A}_2$ satisfies the following equation

$$\nabla^2 \boldsymbol{A}_2(\boldsymbol{r}, t) = \partial_t^2 \boldsymbol{A}_2(\boldsymbol{r}, t) + \sigma \partial_t \boldsymbol{A}_2(\boldsymbol{r}, t) - \boldsymbol{j}(\boldsymbol{r}, t) \tag{8}$$

with the initial conditions

$$\boldsymbol{A}_2(\boldsymbol{r}, t_0) = \boldsymbol{A}_1(\boldsymbol{r}, t_0) \equiv \hat{\boldsymbol{z}}\Phi(\boldsymbol{r}, t_0), \tag{9}$$
$$\partial_t \boldsymbol{A}_2(\boldsymbol{r}, t_0) = \partial_t \boldsymbol{A}_1(\boldsymbol{r}, t_0) \equiv \hat{\boldsymbol{z}}\Psi(\boldsymbol{r}, t_0). \tag{10}$$

I stress that the current density $\boldsymbol{j}$ is due to electric charges outside the plasma. I assumed that permittivity and permeability of QGP is trivial. One can take a more accurate account of medium properties, which would yield more elaborate initial conditions. However, they are not expected to significantly change the final result.

In momentum space Eq. (8) and the corresponding initial conditions (9),(10) read

$$-k^2 \boldsymbol{A}_{2\boldsymbol{k}}(t) = \partial_t^2 \boldsymbol{A}_{2\boldsymbol{k}}(t) + \sigma \partial_t \boldsymbol{A}_{2\boldsymbol{k}}(t) - ev\hat{\boldsymbol{z}} e^{-ik_z vt}, \tag{11}$$

$$\boldsymbol{A}_{2\boldsymbol{k}}(t_0) = \hat{\boldsymbol{z}}\Phi_{\boldsymbol{k}}(t_0) = \frac{ev\hat{\boldsymbol{z}}}{k_z^2/\gamma^2 + k_\perp^2} e^{-ik_z vt_0}, \tag{12}$$

$$\partial_t \boldsymbol{A}_{2\boldsymbol{k}}(t_0) = \hat{\boldsymbol{z}}\Psi_{\boldsymbol{k}}(t_0) = -ik_z v \frac{ev\hat{\boldsymbol{z}}}{k_z^2/\gamma^2 + k_\perp^2} e^{-ik_z vt_0}. \tag{13}$$

To solve (11), I first consider the corresponding homogeneous equation

$$-k^2 a_{\boldsymbol{k}}(t) = \partial_t^2 a_{\boldsymbol{k}}(t) + \sigma \partial_t a_{\boldsymbol{k}}(t) \,, \tag{14}$$

Seeking its solution in the form $a_{\boldsymbol{k}} \propto e^{-i\omega t}$ I find, upon substitution into (14), that ω must obey one the following dispersion relations

$$\omega = \omega_{\pm} = -\frac{i\sigma}{2} \pm \sqrt{k^2 - \frac{\sigma^2}{4}} \,. \tag{15}$$

Thus, the general solution of the homogeneous equation (14), which describes propagation of the initial conditions, reads

$$a_{\boldsymbol{k}}(t) = \alpha e^{-i\omega_+(t-t_0)} + \beta e^{-i\omega_-(t-t_0)} \,, \tag{16}$$

where α and β are constants to be determined from the initial conditions (12) and (13). The particular solution due to the external current density is of the form $A_{2\boldsymbol{k}} \propto \delta e^{-ik_z vt}$, where δ is found upon substitution into (11):

$$\delta = \frac{ev}{k^2 - k_z^2 v^2 - ik_z v\sigma} \,. \tag{17}$$

Thus, the general solution to (11) is

$$\boldsymbol{A}_{2\boldsymbol{k}} = \hat{\boldsymbol{z}} \left\{ \alpha e^{-i\omega_+(t-t_0)} + \beta e^{-i\omega_-(t-t_0)} + \frac{ev}{k^2 - k_z^2 v^2 - ik_z v\sigma} e^{-ik_z vt} \right\} \,. \tag{18}$$

Applying the initial conditions (12) and (13) I can fix α and β. The final result is

$$\begin{aligned} \boldsymbol{A}_{2\boldsymbol{k}} = \hat{\boldsymbol{z}} \Bigg\{ &\delta \left[\left(\frac{\omega_- - k_z v}{\omega_+ - \omega_-} e^{-i\omega_+(t-t_0)} - \frac{\omega_+ - k_z v}{\omega_+ - \omega_-} e^{-i\omega_-(t-t_0)} \right) e^{-ik_z vt_0} + e^{-ik_z vt} \right] \\ &+ \frac{1}{i(\omega_+ - \omega_-)} \Phi_{\boldsymbol{k}} \left[-i\omega_- e^{-i\omega_+(t-t_0)} + i\omega_+ e^{-i\omega_-(t-t_0)} \right] \\ &+ \frac{1}{i(\omega_+ - \omega_-)} \Psi_{\boldsymbol{k}} \left[-e^{-i\omega_+(t-t_0)} + e^{-i\omega_-(t-t_0)} \right] \Bigg\} \,. \end{aligned} \tag{19}$$

Fourier transformation to the configuration space yields exact analytical solution to the initial value problem (8)–(10). Analytical and numerical evaluations of the integral over $\boldsymbol{k}$ are challenging. Fortunately, in the ultra-relativistic limit $\gamma \gg 1$, which is relevant for the relativistic heavy-ion collisions, expression for the vector potential (19) significantly simplifies [6]. This is the subject of the next section.

IV. DIFFUSION APPROXIMATION

For an ultra-relativistic charge moving along the trajectory $z = vt$, $\partial_t^2 - \partial_z^2 \sim k_z^2/\gamma^2 \ll k_\perp^2, \sigma k_z$, which implies $\sigma\gamma \gg k_\perp$ [6]. In this case (8) can be approximated by

$$\nabla_\perp^2 \boldsymbol{A}_2(\boldsymbol{r}, t) = \sigma \partial_t \boldsymbol{A}_2(\boldsymbol{r}, t) - \boldsymbol{j}(\boldsymbol{r}, t) \,. \tag{20}$$

This approximation holds even in the case of time-dependent conductivity, provided that such dependence is adiabatic, which is a reasonable approximation for the realistic plasma. Since (20) is of the first order in the time derivative, it requires only one initial condition

$$\boldsymbol{A}_2(\boldsymbol{r}, t_0) = \boldsymbol{A}_1(\boldsymbol{r}, t_0) = \hat{\boldsymbol{z}} \Phi(\boldsymbol{r}, t_0) \,. \tag{21}$$

I can solve the initial value problem (20)-(21) for an arbitrary time-dependence of the conductivity $\sigma(t)$. Introducing a new "time"-variable λ according to

$$\lambda(t) = \int_{t_0}^t \frac{dt'}{\sigma(t')} \tag{22}$$

and transferring (20) to the momentum space I obtain

$$-k_\perp^2 \boldsymbol{A}_{2\boldsymbol{k}} = \partial_\lambda \boldsymbol{A}_{2\boldsymbol{k}} - \boldsymbol{j}_{\boldsymbol{k}} \,. \tag{23}$$

The corresponding homogeneous equation (i.e. (23) with $\boldsymbol{j}_{\boldsymbol{k}} = 0$) is solved by

$$\boldsymbol{a}_{\boldsymbol{k}}(\lambda) = \hat{\boldsymbol{z}} C e^{-k_\perp^2 \lambda} \,, \tag{24}$$

where C is a constant. To derive a particular solution, I treat C as a function of λ and plug into (23). I get

$$C = ev \int_0^\lambda d\lambda' e^{k_\perp^2 \lambda' - ik_z vt(\lambda')} + D \,. \tag{25}$$

Substituting into (24) I find the general solution to (23)

$$\boldsymbol{A}_{2\boldsymbol{k}}(t) = \hat{\boldsymbol{z}} \left\{ eve^{-k_\perp^2 \lambda} \int_0^\lambda d\lambda' e^{k_\perp^2 \lambda' - ik_z vt(\lambda')} + De^{-k_\perp^2 \lambda} \right\} \,. \tag{26}$$

Since $\lambda(t_0) = 0$, the initial condition (21) implies that $D = \Phi_{\boldsymbol{k}}(\boldsymbol{r}, t_0)$. So finally,

$$\boldsymbol{A}_{2\boldsymbol{k}}(t) = \hat{\boldsymbol{z}} \left\{ eve^{-k_\perp^2 \lambda(t)} \int_{t_0}^t \frac{dt'}{\sigma(t')} e^{k_\perp^2 \lambda(t') - ik_z vt'} + \Phi_{\boldsymbol{k}} e^{-k_\perp^2 \lambda(t')} \right\} \,. \tag{27}$$

In a particular case of constant electrical conductivity (27) simplifies to

$$\boldsymbol{A}_{2\boldsymbol{k}}(t) = \hat{\boldsymbol{z}} \left\{ \frac{ev}{\sigma} \frac{1}{\frac{k_\perp^2}{\sigma} - ik_z v} \left(e^{-ik_z vt} - e^{-\frac{k_\perp^2}{\sigma}(t-t_0)} e^{-ik_z vt_0} \right) + \Phi_{\boldsymbol{k}} e^{-\frac{k_\perp^2}{\sigma}(t-t_0)} \right\} \,. \tag{28}$$

This expression can be derived directly from (19), but the approach described in this section is more straightforward. Fourier transformation to the configuration space

$$\boldsymbol{A}_2(\boldsymbol{r}, t) = \int \frac{d^2k_\perp}{(2\pi)^2} \int_{-\infty}^{+\infty} \frac{dk_z}{2\pi} e^{i\boldsymbol{k}_\perp \cdot \boldsymbol{b} + ik_z z} \boldsymbol{A}_{2\boldsymbol{k}}(t) \tag{29}$$

can be done using the following integrals

$$\int \frac{d^2k_\perp}{(2\pi)^2} \int_{-\infty}^{+\infty} \frac{dk_z}{2\pi} e^{i\boldsymbol{k}_\perp \cdot \boldsymbol{b} + ik_z z} e^{-k_\perp^2 [\lambda(t) - \lambda(t')]} = \frac{\exp\left\{ -\frac{b^2}{4[\lambda(t) - \lambda(t')]} \right\}}{4[\lambda(t) - \lambda(t')]} \delta(z - vt') \,, \tag{30}$$

$$\int \frac{d^2k_\perp}{(2\pi)^2} \int_{-\infty}^{+\infty} \frac{dk_z}{2\pi} e^{i\boldsymbol{k}_\perp \cdot \boldsymbol{b} + ik_z z} e^{-k_\perp^2 \lambda(t)} \frac{ev}{k_z^2/\gamma^2 + k_\perp^2} e^{-ik_z vt_0}$$
$$= \frac{\gamma ev}{4\pi} \int_0^\infty dk_\perp J_0(k_\perp b) e^{-k_\perp^2 \lambda(t) - k_\perp \gamma |z - vt_0|} \,. \tag{31}$$

Substituting (27) into (29), doing integrals (30),(31) and then integrating over t' yields

$$\boldsymbol{A}_2(\boldsymbol{r}, t) = \frac{\hat{\boldsymbol{z}} e}{4\sigma(z/v)} \frac{\exp\left\{ -\frac{b^2}{4[\lambda(t) - \lambda(z/v)]} \right\}}{4[\lambda(t) - \lambda(z/v)]} \theta(tv - z) \theta(z - vt_0)$$
$$+ \frac{\gamma ev \hat{\boldsymbol{z}}}{4\pi} \int_0^\infty dk_\perp J_0(k_\perp b) e^{-k_\perp^2 \lambda(t) - k_\perp \gamma |z - vt_0|} \,. \tag{32}$$

Magnetic field can be calculated as in (7) with the following result

$$\boldsymbol{B}_2 = \boldsymbol{B}_{\text{val}} + \boldsymbol{B}_{\text{init}} \,, \tag{33}$$

where the "valence" $\boldsymbol{B}_{\text{val}}$ and "initial" $\boldsymbol{B}_{\text{init}}$ components are given by

$$e\boldsymbol{B}_{\text{val}}(\boldsymbol{r}, t) = \hat{\boldsymbol{\phi}} \frac{\alpha \pi b}{2\sigma(z/v)[\lambda(t) - \lambda(z/v)]^2} \exp\left\{ -\frac{b^2}{4[\lambda(t) - \lambda(z/v)]} \right\} \theta(tv - z) \theta(z - vt_0) \,, \tag{34}$$

$$e\boldsymbol{B}_{\text{init}}(\boldsymbol{r}, t) = \hat{\boldsymbol{\phi}} \gamma \alpha v \int_0^\infty dk_\perp k_\perp J_1(k_\perp b) \exp\left\{ -k_\perp^2 \lambda(t) - k_\perp \gamma |z - vt_0| \right\} \,. \tag{35}$$

The fine structure constant $\alpha = e^2/(4\pi)$. Note that at $t = t_0$, $\boldsymbol{B}_{\text{val}}$ vanishes whereas $\boldsymbol{B}_{\text{init}}$ yields the initial condition (7). $\boldsymbol{B}_{\text{init}}$ is the field that permits the plasma as it emerges at $t = t_0$ (at which time it coincides with $\boldsymbol{B}_1$) and spreads in it according to (35). Unlike $\boldsymbol{B}_{\text{val}}$, it strongly dependences on the collision energy 2γ (in units of proton mass).

$\boldsymbol{B}_{\text{val}}$ describes induced electromagnetic field generated as a response of QGP to electromagnetic field of the valence charge and builds up starting from $t = t_0$. Because of the two step-functions in (34) that reflect causality, $\boldsymbol{B}_{\text{val}}$ is finite only in the interval $vt_0 \leq z \leq vt$. In particular, it vanishes in the midrapidity $z = 0$. At fixed z satisfying $z \geq vt_0$, $\boldsymbol{B}_{\text{val}}$ emerges when $t = z/v$. An important property of $\boldsymbol{B}_{\text{val}}$ is that its magnitude is independent of energy (since $v \approx 1$).

At early times since the QGP creation viz. $t \gtrsim t_0$, expression in the exponent of (35) is such that $k_\perp^2 \lambda \ll k_\perp \gamma |z - vt_0|$ implying that $\boldsymbol{B}_{\text{init}} \approx \boldsymbol{B}_1$. However, at later times when $k_\perp^2 \lambda \gg k_\perp \gamma |z - vt_0|$, I get

$$e\boldsymbol{B}_{\text{init}} = \hat{\phi}\frac{\gamma\alpha vb\sqrt{\pi}}{8\lambda^{3/2}}e^{-\frac{b^2}{8\lambda}}\left[I_0\left(\frac{b^2}{8\lambda}\right) - I_1\left(\frac{b^2}{8\lambda}\right)\right]. \tag{36}$$

Since $k_\perp b \sim \sqrt{8}$ (which can be seen from J_1 series expansion) and $\lambda \sim (t - t_0)/\sigma$ I estimate that (36) is valid at times t satisfying

$$\frac{t - t_0}{|z - vt_0|} \gg \frac{1}{\sqrt{8}}\gamma\sigma b. \tag{37}$$

At $z = 0$, $b = 7$ fm and $t_0 = 0.2$ fm this implies $t \gg 1$ fm, where I used $\sigma = 5.8$ MeV known from the lattice calculations [13], see also [14–16]. Furthermore, since $b^2/8\lambda \ll 1$ I expand (36) to obtain the late-time behavior of the initial magnetic field

$$e\boldsymbol{B}_{\text{init}} \approx \frac{\gamma\alpha v\sqrt{\pi}b}{8\lambda^{3/2}}\hat{\phi}. \tag{38}$$

For constant σ the late-time dependence (viz. $t \gg t_0$) is $B_{\text{init}} \sim 1/t^{3/2}$. Notice that at late times the "valence" contribution decays as $B_{\text{val}} \sim 1/t^2$. It therefore emerges that the initial magnetic field dominates at early and late times.

V. MAGNETIC FIELD OF TWO COUNTER-PROPAGATING CHARGES

To calculate magnetic field in a heavy-ion collision one considers two sets of Z counter-propagating electric charges distributed according to one of the known nuclear density parameterizations, see e.g. [3]. However, to study the time evolution of magnetic field it suffices to consider just two counter-propagating charges. The geometric symmetry of this configuration is similar to that of the event-average over many heavy-ion collisions at impact parameter b, but drastically reduces the computational time. The configuration that I consider is depicted in Fig. 1.
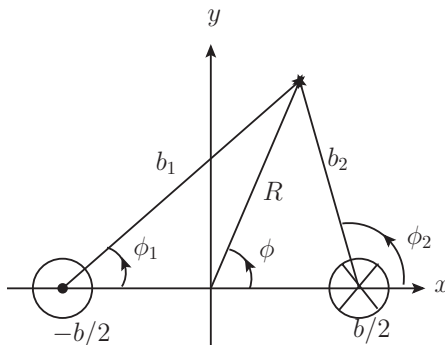

FIG. 1: Two counter-propagating charges e. One charges moves along the positive z-axis at $z = vt$, $x = -b/2$, $y = 0$ while another one moves in the opposite direction at $z = -vt$, $x = b/2$, $y = 0$.

Let $B^{(1)}(\boldsymbol{r}_1, t)$ and $B^{(2)}(\boldsymbol{r}_2, t)$ be magnitudes of the fields of the two charges, each given by (33)–(35). I can express coordinates of the observation point relative to each charge $\boldsymbol{r}_1 = \boldsymbol{b}_1 + \hat{\boldsymbol{z}}z_1$ and $\boldsymbol{r}_2 = \boldsymbol{b}_2 + \hat{\boldsymbol{z}}z_2$ in terms of their

center-of-mass in cylindrical coordinates R, z, ϕ as follows, see Fig. 1

$$b_a = \sqrt{b^2/4 + R^2 + (-1)^a \, bR \cos \phi}, \quad \tan \phi_a = \frac{R \sin \phi}{R \cos \phi - (-1)^a \, b/2}, \quad z_a = vt + (-1)^a \, z. \tag{39}$$

where $a = 1, 2$ labels the charges. Noting that $\boldsymbol{B}^{(a)} \propto \hat{\boldsymbol{\phi}}_a$ and expressing $\hat{\boldsymbol{\phi}}_a$ in terms of $\hat{\boldsymbol{b}}$ and $\hat{\boldsymbol{\phi}}$ I obtain magnetic field in terms of the center-of-mass frame coordinates

$$\begin{aligned}
\boldsymbol{B} = &\hat{\boldsymbol{b}}[B^{(1)}(\boldsymbol{r}_1, t) \sin(\phi - \phi_1) + B^{(2)}(\boldsymbol{r}_2, t) \sin(\phi - \phi_2)] \\
&+ \hat{\boldsymbol{\phi}}[B^{(1)}(\boldsymbol{r}_1, t) \cos(\phi - \phi_1) + B^{(2)}(\boldsymbol{r}_2, t) \cos(\phi - \phi_2)],
\end{aligned} \tag{40}$$

where $\boldsymbol{r}_a$ and ϕ_a are replaced as indicated in (39). The result is shown in Fig. 2–Fig. 5 in terms of a dimensionless and unit-independent quantity eB/m_π^2. In all figures impact parameter is $b = 1$ fm, observation point is at $\phi = \pi/2$, $R = 7$ fm (i.e. $x = 0$ and $y = 7$ fm), and $\gamma = 100$ (except Fig. 4). Also indicated is the pseudorapidity $\eta = -\ln[-(z/R) + \sqrt{(z/R)^2 + 1}]$. Solid lines indicate the total magnetic field B, dashed lines represent the contribution of the initial condition B_{init} and dotted lines stand for the contribution of the valence charges B_{val}. As discussed at the end of the previous section valence charge contribution decreases with time faster than that of the initial condition.
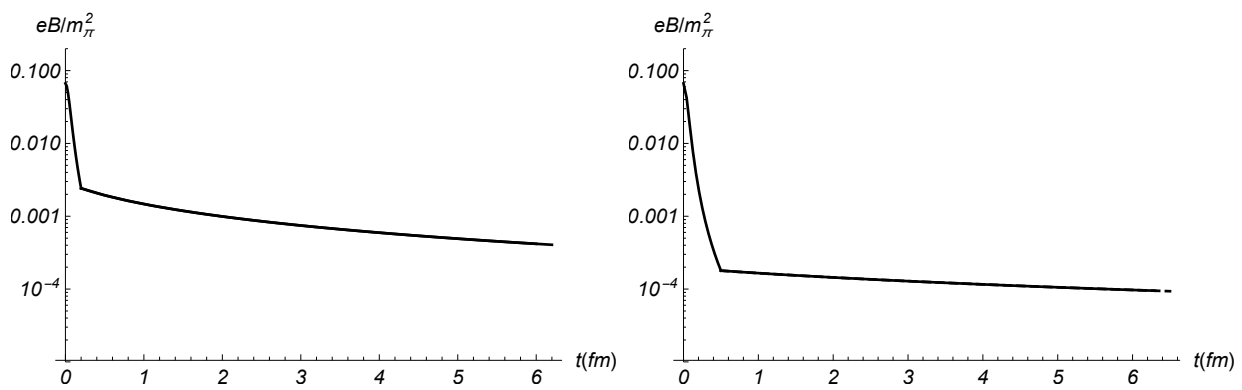

FIG. 2: Magnetic field in units of m_π^2/e. $\sigma = 5.8$ MeV, $z = 0$ fm ($\eta = 0$). Left panel: $t_0 = 0.2$ fm, right panel: $t_0 = 0.5$ fm. Valence current does not contribute at all ($B_{\text{val}} = 0$).
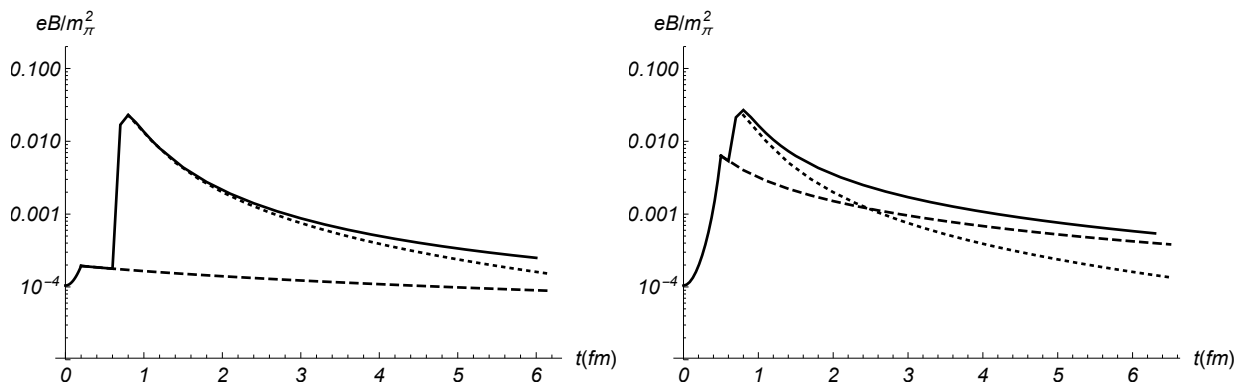

FIG. 3: Magnetic field in units of m_π^2/e. $\sigma = 5.8$ MeV, $z = 0.6$ fm ($\eta = 0.086$). Left panel: $t_0 = 0.2$ fm, right panel: $t_0 = 0.5$ fm. Solid, dashed and dotted lines stand for B, B_{init} and B_{val}.

Fig. 2–Fig. 4 depict magnetic field at constant electrical conductivity $\sigma = 5.8$ MeV [13]. In Fig. 2 I compare magnetic field that is generated when QGP emerges at $t_0 = 0.2$ fm and at $t_0 = 0.5$ fm. Since magnetic field in vacuum decreases as $1/t^3$, see (7), the late emergence of conducting medium means that the magnitude of the field in the former case is about 15 times larger than in the later. In both cases time-dependence of magnetic field in plasma is mild. Because of the step functions in (34) magnetic field at midrapidity $z = 0$ is entirely due to the initial field B_{init}.

Fig. 3 is similar to Fig. 2 except that $z = 0.6$ fm unlocking the "valence" contribution. Being independent of the initial value of magnetic field at t_0 the "valence" contribution rapidly increases to its maximal value, that can be

determined from (34) [12]. It then decreases at larger t and becomes smaller than B_{init}. Sharp lines seen in Fig. 3 indicate that the transition dynamics near $t = t_0$ is not fully captured by the diffusion approximation.

Energy dependence of magnetic field between the RHIC and LHC energies can be seen in Fig. 4. B_{init} grows approximately proportional to the collision energy γ, whereas B_{val} is energy independent. Thus, at the LHC magnetic field induced by valence charges is negligible.
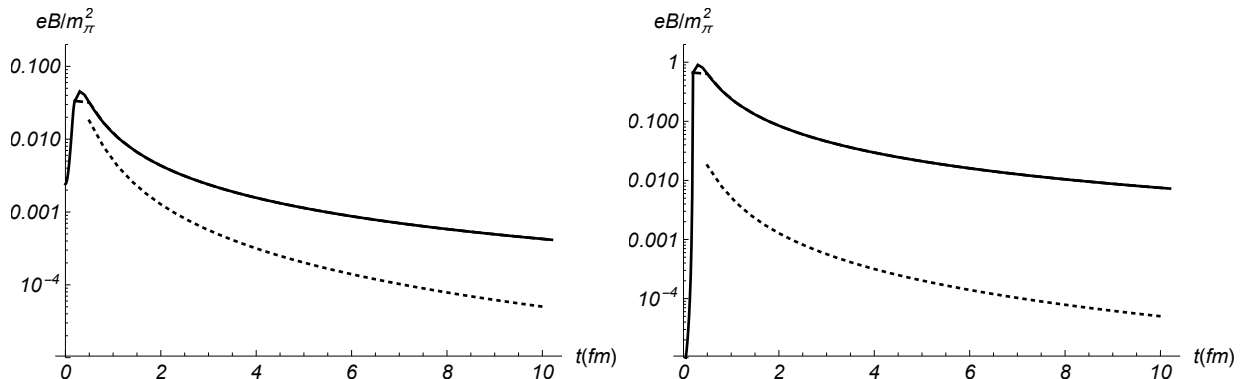

FIG. 4: Magnetic field in units of m_π^2/e. $\sigma = 5.8$ MeV, $z = 0.2$ fm $t_0 = 0.2$ fm. Solid, dashed and dotted lines stand for B, B_{init} and B_{val}. Left panel: $\gamma = 100$ (RHIC), right panel: $\gamma = 2000$ (LHC).

So far I considered only the case of constant electrical conductivity. In practice, however electrical conductivity is time-dependent. To see the impact of σ time-dependence on the time evolution of magnetic field I consider two models. In model A I assume that QGP emerges instantly at $t = t_0$ with $\sigma = 5.8$ MeV and then cools down as it expands according to the Bjorken scenario [17]. Namely, expansion is supposed to be isentropic $nV = \text{const}$, where n is the particle number density and V is plasma volume. Since $n \sim T^3$ and at early times expansion is one-dimensional $V \sim t$ it follows that $T \propto t^{-1/3}$. Since $\sigma(t) \propto T$ I conclude that $\sigma(t) \sim t^{-1/3}$. Thus a reasonable model for time dependence of electrical conductivity is

$$\sigma(t) = \frac{\sigma}{2^{-1/3}(1 + t/t_0)^{1/3}}, \quad \text{Model A.} \tag{41}$$

Another possibility is that the QGP does not appear as a thermal medium right away at $t = t_0$, rather it takes time τ until the conductivity reaches its equilibrium value σ. This can be described as

$$\sigma(t) = \sigma \left(1 - e^{-t/\tau}\right), \quad \text{Model B.} \tag{42}$$

I set conservatively $\tau = 1$ fm. Note that I cannot let $\sigma(t)$ vanish at $t = t_0$ because that would violate the diffusion approximation that lead to (20). However, (42) insures that $\sigma(t_0) \ll \sigma$.

In Fig. 5 I contrast the two models. Similar calculation at constant conductivity is shown in the left panel of Fig. 4. I observe that time-dependence (41) (model A) significantly reduces magnetic field at later times. As far as model B is concerned, time dependence (42) affects mostly B_{val} because it directly depends on $\sigma(t)$, whereas B_{init} depends only on $\lambda(t)$, see (34),(35). Model B has minor effect on the total magnetic field, although one can certainly find regions in space-time where its effect is more pronounced. What actually matters is the initial time t_0 at which one can treat the produced particle system as a medium. As long as conductivity is large enough at later times, magnetic field is fairly insensitive to the precise QGP dynamics.

VI. SUMMARY

Just before the QGP emerges, the interaction region is permitted by the primordial electromagnetic field created by valence charges of two heavy-ions. At the initial time t_0 this magnetic field smoothly connects to the magnetic field in plasma and evolves according to the Maxwell equations in the electrically conducting medium. In addition to this "initial" magnetic field, there is another "valence" contribution that arises from the external valence electric charges inducing currents in the QGP. It has been tacitly assumed that the former contribution is not important [6]. In this paper I argued to the contrary, that the initial magnetic field dominates at very early and later times and increases much faster with the collision energy than the "valence" contribution.
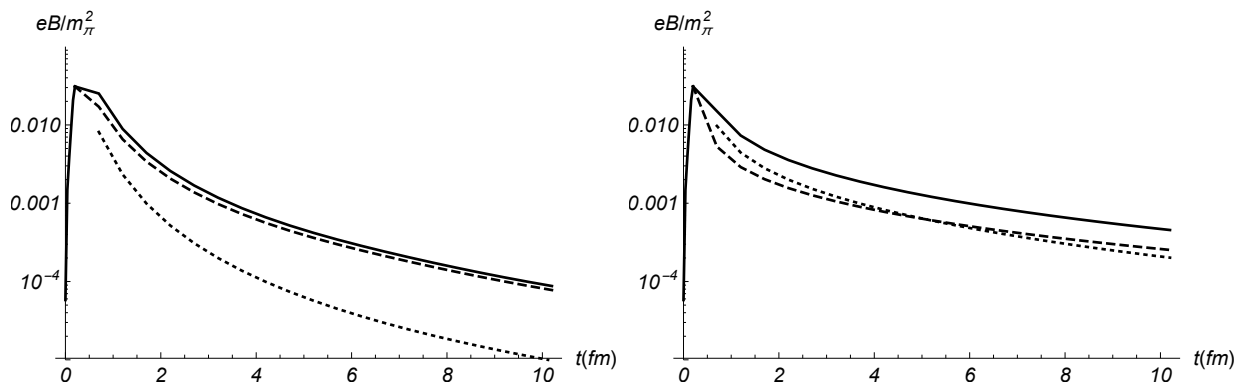
FIG. 5: Magnetic field in units of m_π^2/e. $z = 0.2$ fm $t_0 = 0.2$ fm. Left panel: model A. Right panel: model B. Solid, dashed and dotted lines stand for B, B_{init} and B_{val}.

I also studied the effect of time dependence of electrical conductivity and concluded that at early times it has a rather minor effect on the field strength, as long as the produced particle system can be treated as a medium at early enough time. However, towards the later times of plasma evolution, time-dependence of electrical conductivity plays an important role. In the Bjorken scenario it leads to much weaker fields as compared to the constant conductivity case.

I considered the case of two counter-propagating charges that gives an accurate picture for the time dependence of the event-averaged fields in heavy-ion collisions. Scaling the result with Z I can obtain an estimate of the magnetic field strength in heavy-ion collisions. Calculating the spatial distribution requires an accurate account of the exact nuclear geometry, which is not difficult using the results reported in this paper.

Acknowledgments

[1] V. Skokov, A. Y. Illarionov and V. Toneev, "Estimate of the magnetic field strength in heavy-ion collisions," Int. J. Mod. Phys. A **24**, 5925 (2009).
[2] K. Tuchin, "Synchrotron radiation by fast fermions in heavy-ion collisions," Phys. Rev. C **82**, 034904 (2010) [Erratum-ibid. C **83**, 039903 (2011)].
[3] A. Bzdak and V. Skokov, "Event-by-event fluctuations of magnetic and electric fields in heavy ion collisions," Phys. Lett. B **710**, 171 (2012).
[4] V. Voronyuk, V. D. Toneev, W. Cassing, E. L. Bratkovskaya, V. P. Konchakovski, S. A. Voloshin, "(Electro-)Magnetic field evolution in relativistic heavy-ion collisions," Phys. Rev. **C83**, 054911 (2011).
[5] W. -T. Deng and X. -G. Huang, "Event-by-event generation of electromagnetic fields in heavy-ion collisions," Phys. Rev. C **85**, 044907 (2012).
[6] K. Tuchin, "Time and space dependence of the electromagnetic field in relativistic heavy-ion collisions," Phys. Rev. C **88**, no. 2, 024911 (2013)
[7] L. McLerran and V. Skokov, "Comments About the Electromagnetic Field in Heavy-Ion Collisions," Nucl. Phys. A **929**, 184 (2014)
[8] B. G. Zakharov, "Electromagnetic response of quark-gluon plasma in heavy-ion collisions," Phys. Lett. B **737**, 262 (2014)
[9] K. Itakura, Y. V. Kovchegov, L. McLerran and D. Teaney, "Baryon stopping and valence quark distribution at small x," Nucl. Phys. A **730**, 160 (2004)
[10] D. Kharzeev, "Can gluons trace baryon number?," Phys. Lett. B **378**, 238 (1996)
[11] P. F. Kolb and U. W. Heinz, "Hydrodynamic description of ultrarelativistic heavy ion collisions," In *Hwa, R.C. (ed.) et al.: Quark gluon plasma* 634-714
[12] K. Tuchin, "Particle production in strong electromagnetic fields in relativistic heavy-ion collisions," Adv. High Energy Phys. **2013**, 490495 (2013)
[13] H.-T. Ding, A. Francis, O. Kaczmarek, F. Karsch, E. Laermann and W. Soeldner, "Thermal dilepton rate and electrical conductivity: An analysis of vector current correlation functions in quenched lattice QCD," Phys. Rev. D **83**, 034504 (2011)

[14] G. Aarts, C. Allton, J. Foley, S. Hands and S. Kim, "Spectral functions at small energies and the electrical conductivity in hot, quenched lattice QCD," Phys. Rev. Lett. **99**, 022002 (2007)

[15] A. Amato, G. Aarts, C. Allton, P. Giudice, S. Hands and J. I. Skullerud, "Transport coefficients of the QGP," PoS LATTICE **2013**, 176 (2014)

[16] W. Cassing, O. Linnyk, T. Steinert and V. Ozvenchuk, "On the electric conductivity of hot QCD matter," Phys. Rev. Lett. **110**, 182301 (2013)

[17] J. D. Bjorken, "Highly Relativistic Nucleus-Nucleus Collisions: The Central Rapidity Region," Phys. Rev. D **27**, 140 (1983).